

Reconstruction of Backbone Curves for Snake Robots

Tianyu Wang^{1,*}, Bo Lin^{2,*}, Baxi Chong³, Julian Whitman¹, Matthew Travers¹,
Daniel I. Goldman³, Greg Blekherman², Howie Choset¹

Abstract—Snake robots composed of alternating single-axis pitch and yaw joints have many internal degrees of freedom, which make them capable of versatile three-dimensional locomotion. Often, snake robot motions are planned kinematically by a chronological sequence of continuous backbone curves that capture desired macroscopic shapes of the robot. However, as the geometric arrangement of single-axis rotary joints creates constraints on the rotations in the robot, it is challenging for the robot to reconstruct an arbitrary 3-D curve. When the robot configuration does not accurately achieve the desired shapes defined by these backbone curves, the robot can have undesired contact with the environment, such that the robot does not achieve the desired motion. In this work, we propose a method for snake robots to reconstruct desired backbone curves by posing an optimization problem that exploits the robot’s geometric structure. We verified that our method enables accurate curve-configuration conversions through its applications to commonly used 3-D gaits. We also demonstrated via robot experiments that 1) our method results in smooth locomotion on the robot; 2) our method allows the robot to approach the numerically predicted locomotive performance of a sequence of continuous backbone curve.

I. INTRODUCTION

Snake robots are a class of hyper-redundant mechanisms capable of achieving different types of locomotion by coordinated flexing of their bodies. One of the well-established snake robot designs is composed of alternating one degree of freedom (DOF) pitch and yaw bending joints (as shown in Fig. 1), which allows three-dimensional versatile motion [1]–[4]. Such a robot design is also called “twist-free” since it does not have direct actuation of the twist (rotation about the longitudinal axis of the body) DOF [5]. Inspired by the shapes of biological snakes with many vertebrae, finite-length continuous backbone curves are designed to capture desired macroscopic shapes of robots [6], [7]. Often, the motion of a snake robot is planned kinematically by a chronological sequence of backbone curves [8], [9]. Some backbone curves have been shown by prior work to generate effective, biologically-inspired, locomotion such as lateral undulation, sidewinding, and sinus lifting [6], [10], [11]. In order to replicate those motions on the physical robot,

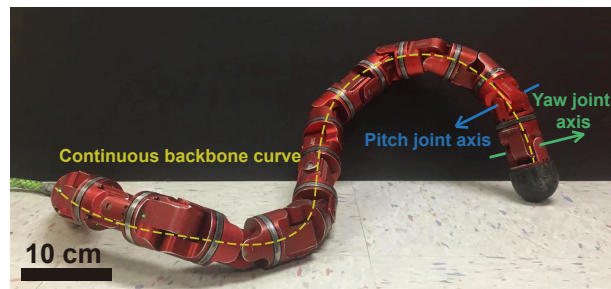


Fig. 1: An example of a “twist-free” snake robot design with alternating single-axis pitch and yaw joints.

we have to match the shape of a robot made up of discrete segments to the continuous curves. These backbone curves lie in three-dimensional space, but the geometric arrangement of single-axis rotary joints creates constraints on the rotations in the robot, making this shape-matching problem challenging for twist-free snake robots. During locomotion, the robot can have undesired contact with the environment when the body shape does not match the desired backbone curve, such that the robot cannot generate the desired motion. This paper presents a method for twist-free snake robots to accurately reconstruct desired 3-D backbone curves via a constrained optimization problem. This enables the robot to locomote effectively by following a sequence of backbone curves.

In prior work, a widely employed method to reconstruct 3-D continuous backbone curves with snake robot configurations is to decompose the 3-D curve into 2-D sub-curves and separately prescribe the pitch and yaw joint angles by parameterized sinusoidal functions according to 2-D sub-curves [12]–[14]. This method simplifies the conversion process and is easily implemented. However it often neglects the intrinsic twisting properties in the given 3-D curve [15], and predefined sinusoidal functions often cannot provide good approximations to sub-curves, which can lead to discrepancies between the resultant robot configuration and the desired backbone curve. Another branch of approaches to the reconstruction problem is to discretize the curve by fitting piece-wise linear segments to the continuous finite-length curve with optimization tools [16]–[18]. However, such approaches often assume two or more DOFs of rotation capability at each joint, preventing their direct application to the alternating-rotation robot geometry. A method introduced in [8] unified these two types of approaches by first fitting the robot configurations to the curves with the optimization algorithm, then smoothing out the fitted joint angles over time with parameterized sinusoidal functions. The optimization algorithm allows conversions from individual 3-D backbone curves to individual robot configurations but

*These authors contributed equally

¹Tianyu Wang, Julian Whitman, Matthew Travers and Howie Choset are with the Robotics Institute, Carnegie Mellon University, Pittsburgh, PA 15213, USA. {tianyuw2, jwhitman, mtravers, choset}@andrew.cmu.edu

²Bo Lin and Greg Blekherman are with the School of Mathematics, Georgia Institute of Technology, and Southeast Center for Mathematics and Biology (SCMB), Atlanta, GA 30332, USA. {bo.lin, greg}@math.gatech.edu

³Baxi Chong and Daniel I. Goldman are with the School of Physics, Georgia Institute of Technology, Atlanta, GA 30332, USA. bchong9@gatech.edu, daniel.goldman@physics.gatech.edu.

the output joint angles are not continuous over time so the smoothing step is necessary. However, the smoothing process does not directly consider the desired backbone curve, such that the joint angles after smoothing may no longer fit the given curves.

In this work, we propose a method for snake robots with an alternating single-axis pitch and yaw joints design to reconstruct desired 3-D backbone curves. We develop the constrained optimization algorithm in such a way that it exploits the geometric structure of the robot. We test our reconstruction approach on 3-D backbone curves common in the literature [6], [13], [19], [20]. By comparing individual robot configurations with the given backbone curves, we show that our method allows the robot configurations to match the given curves more precisely than the previous method. We also conduct physical robot experiments where we apply our method in real-time during the process of robot executing 3-D gaits. We experimentally validate that our method ensures that small changes in the desired backbone curves only result in small changes in the robot configuration, thus the robot commanded joint angles vary smoothly. We then demonstrate that our method allows the robot to approach the numerically predicted motion of a sequence of desired continuous backbone curves.

II. RELATED WORK

There are two primary approaches in prior work for reconstruction of the 3-D continuous backbone curves with discrete robot configurations in snake robot locomotion.

The first dominant approach to the configuration reconstruction problem is to decompose the 3-D curve into 2-D sub-curves and derive pitch and yaw joint angles separately with simple heuristics. Widely employed in snake robot gait design and control for the robots an alternating single-axis pitch and yaw joints design [12]–[14], this approach first decomposes the desired 3-D backbone curves to two 2-D sub-curves in the vertical plane and the horizontal plane, and fits the vertical and horizontal body shape of the robot to the sub-curves by prescribing the pitch and yaw joint angles with two parameterized sinusoidal equations. This approach is simple to implement, but, during the decomposition process the twisting properties of the desired curves are often neglected, and predefined parameterized sinusoidal equations often cannot provide good approximations to sub-curves. Thus, the given curves cannot be fully replicated, leading to the errors between the robot configurations and the desired curves.

The other dominant approach to the reconstruction problem is discretization of the 3-D curve by fitting piece-wise linear segments to the continuous finite-length curve with optimization tools. Chirikjian and Burdick [16] proposed modal functions for describing arbitrary 3-D backbone curves and developed algorithms for fitting discrete serial mechanisms to desired curves. Mochiyama et al. [17] considered the discretization problem as a shape-tracking control problem by deriving a control law for the joints such that the robot converges to the desired shape. Anderson [18] derived analytical expressions for the relative orientations of the links in the

configuration with a bisection search method. However, these approaches assume a mechanism with universal joints, i.e., at least two intersecting rotation axes at each joint, making it challenging to directly implement these approaches on the alternating-rotation robot geometry.

Hatton and Choset [8] proposed a method to solve the reconstruction problem for the snake robots with alternating-rotation geometry by combining the two major types of approaches. First, an optimization problem was formulated that fixed one end of the robot and consecutively optimized joint angles to “pull” the rest of links towards the desired backbone curve. Solving this optimization problem produces conversions from individual 3-D backbone curves to individual robot configurations. However, when applied to a chronological sequence of the desired backbone curve, the joint angles outputs were not smooth over time, which cannot produce a continuous motion on the robot. To address the discontinuity in the optimizer outputs, a post-processing smoothing step was used in which, parameterized sinusoidal equations were fit to the trajectories that the optimization algorithm produced. However, since the smoothing process does not directly consider the desired backbone curve, errors often emerge in the process of fitting the joint angle trajectories to sinusoidal functions, which can result in shapes that no longer fit the desired backbone curves well.

III. METHODS

We address the problem of converting from a 3-D continuous backbone curve to an alternating-pitch-and-yaw robot configuration by posing an optimization problem that exploits the geometric structure of the robot to optimize the robot’s pitch and yaw rotations. We divide our reconstruction strategy into three steps: 1) sampling the desired joint positions in the robot’s work-space based on the given backbone curve, 2) deriving the constraints based on the robot’s geometric structure, designing the objective function, and running an optimization algorithm to obtain optimal joint positions in work-space, and 3) translating the optimal joint positions in work-space to joint angles in joint space that can be executed by the robot.

A. Sampling the backbone curve

In gait design or motion planning for a snake robot, a finite-length continuous backbone curve defines the robot body’s desired shape. To simplify the optimization process without losing the shape properties of the given 3-D backbone curve, we sample a set of points from the curve. The 3-D Cartesian coordinates of the samples are denoted by C_0, C_1, \dots, C_{n+1} , where n is the number of joints on the robot and $C_i = [C_{i,x}, C_{i,y}, C_{i,z}]^T \in \mathbb{R}^3$. C_0 and C_{n+1} are the anterior and posterior ends of the curve, and C_1, \dots, C_n evenly divide the curve into $(n + 1)$ segments with the same arc length. Thus, samples C_i work as the desired positions for the robot joints (C_1 to C_n) and anterior and posterior ends of the robot (C_0 and C_{n+1}).

B. Robot joint position optimization

We first construct the objective function for the optimization problem. We use $(n + 2)$ coordinates $C'_0, C'_1, \dots, C'_{n+1}$ to denote the positions for the anterior end of the robot, n joints of the robot, and the posterior end of the robot. We can thus find the optimal robot configuration by minimizing the objective function

$$\sum_{i=0}^{n+1} \|C_i - C'_i\|^2, \quad (1)$$

i.e., the sum of squares of distances from n joints and two ends of the robot to the corresponding samples on the desired backbone curve.

We then derive the constraints for the optimization problem based on the geometric structure of the robot. For convenience we denote the $(n + 1)$ links by vectors $\mathbf{j}'_i = C'_i - C'_{i-1}$ for $1 \leq i \leq n + 1$ pointing from one joint center to the next. At each joint, the two links \mathbf{j}'_i and \mathbf{j}'_{i+1} belong to the same rotational plane P_i ($1 \leq i \leq n$). To describe the direction of the planes P_i , we associate a unit normal vector $\mathbf{n}_i \in \mathbb{R}^3$ to each of them, which yields a constraint

$$(i) \quad \|\mathbf{n}_i\| = 1 \text{ for } 0 \leq i \leq n + 1.$$

The robot geometry of alternating pitch and yaw joints implies that any two consecutive rotational planes are orthogonal in \mathbb{R}^3 , yielding

$$(ii) \quad \mathbf{n}_i \cdot \mathbf{n}_{i+1} = 0 \text{ for } 0 \leq i \leq n.$$

For $1 \leq i \leq n$, the two links \mathbf{j}'_i and \mathbf{j}'_{i+1} both belong to the plane P_i and the normal vector \mathbf{n}_i is orthogonal to P_i . Thus \mathbf{n}_i is orthogonal to both \mathbf{j}'_i and \mathbf{j}'_{i+1} . Now for $2 \leq i \leq n$, the three vectors $\mathbf{j}'_i, \mathbf{n}_i, \mathbf{n}_{i-1}$ are pairwise orthogonal. Therefore \mathbf{j}'_i is parallel to the cross product $\mathbf{n}_{i-1} \times \mathbf{n}_i$. Thus we have the constraint that

$$(iii) \quad C'_i - C'_{i-1} = \mathbf{j}'_i = l \cdot (\mathbf{n}_{i-1} \times \mathbf{n}_i) \text{ for } 1 \leq i \leq n,$$

where l is the length of each link.

Suppose that we have the vectors \mathbf{j}'_i fixed, then the internal shape of the robot is determined, and the value of the objective function will only depend on the choice of C'_i . For convenience, we let $d_i = C_i + (C'_0 - C'_i)$, then the objective function becomes:

$$\begin{aligned} \sum_{i=0}^{n+1} \|C_i - C'_i\|^2 &= \sum_{i=0}^{n+1} ((C'_0 - d_i) \cdot (C'_0 - d_i)) \\ &= \sum_{i=0}^{n+1} [C'_0 \cdot C'_0 - 2C'_0 \cdot d_i + d_i \cdot d_i] \\ &= (n+2)C'_0 \cdot C'_0 - 2C'_0 \cdot \left(\sum_{i=0}^{n+1} d_i \right) + \sum_{i=0}^{n+1} (d_i \cdot d_i) \\ &= (n+2) \left(C'_0 - \frac{\sum_{i=0}^{n+1} d_i}{n+2} \right) \cdot \left(C'_0 - \frac{\sum_{i=0}^{n+1} d_i}{n+2} \right) \\ &\quad + \left[\sum_{i=0}^{n+1} (d_i \cdot d_i) - \frac{1}{n+2} \left(\sum_{i=0}^{n+1} d_i \right) \cdot \left(\sum_{i=0}^{n+1} d_i \right) \right]. \end{aligned}$$

The term in the last square bracket is a constant, therefore the objective function attains the minimum if and only if $C'_0 =$

$\frac{\sum_{i=0}^{n+1} d_i}{n+2}$, which is equivalent to $\sum_{i=0}^{n+1} C'_i = \sum_{i=0}^{n+1} C_i$. As a necessary mathematical constraint that ensures the objective function to attain the minimum, we have

$$(iv) \quad \sum_{i=0}^{n+1} C'_i = \sum_{i=0}^{n+1} C_i.$$

A physical interpretation of this mathematical constraint is that the centroid of n joints and two ends of the robot should overlap with the centroid of their corresponding samples on the desired backbone curve.

Now we have formalized an optimization problem that exploits the geometric structure of the robot

$$\begin{aligned} &\underset{C'_i}{\text{minimize}} \quad \sum_{i=0}^{n+1} \|C_i - C'_i\|^2 \\ &\text{subject to} \quad \text{constraints (i), (ii), (iii) and (iv).} \end{aligned}$$

The constrained nonlinear optimization problem can be solve by standard gradient-descent algorithms such as MATLAB's built-in function `fmincon` [21]. This implementation gives a local minimum of the objective function and it works well in our experiments. Alternatively, since this is a polynomial optimization problem, the sum-of-square hierarchy [22] can be applied and it produces certified results.

C. Joint angle translation

The output of our optimization procedure are the coordinates $C'_0, C'_1, \dots, C'_{n+1} \in \mathbb{R}^3$, which denote the optimal positions for n joints, the anterior and the posterior ends of the robot in the work-space. We translate the coordinates to the robot joint angles in the joint space so that the result can be implemented on the physical robot. The absolute value of the joint angle is characterized by the inner product of two consecutive links at the joint. The orientation of the rotations within the plane P_i can be specified by the direction of the normal vector \mathbf{n}_i , which is known after solving the optimization problem.

IV. RESULTS

A. Quality of backbone curve-robot configuration conversion

We first tested the proposed 3-D curve reconstruction method on the virtual twist-free alternating-rotation robot model to evaluate the quality of converting the desired backbone curve to the robot configuration. To verify the effectiveness of the reconstruction on different types of 3-D backbone curves, we tested it on the backbone curves for three widely studied 3-D gaits – sidewinding [10], [13], [14], sinus lifting [11], [19], and helical rolling [20], [23]. As a comparison, we also performed the approach that is commonly used in the snake robots with an alternating-rotation geometry – prescribing the pitch and yaw joint angles with two parameterized sinusoidal equations (hereafter we refer to this approach as “the previous method”), as in [8], [12]–[14] discussed in Section II. We measured the discrepancies between the robot configurations by our method and the desired curves and the discrepancies between the robot configurations by the previous method and the desired curves. The discrepancy between the robot configuration and the desired curve is evaluated by the sum of squares distances error

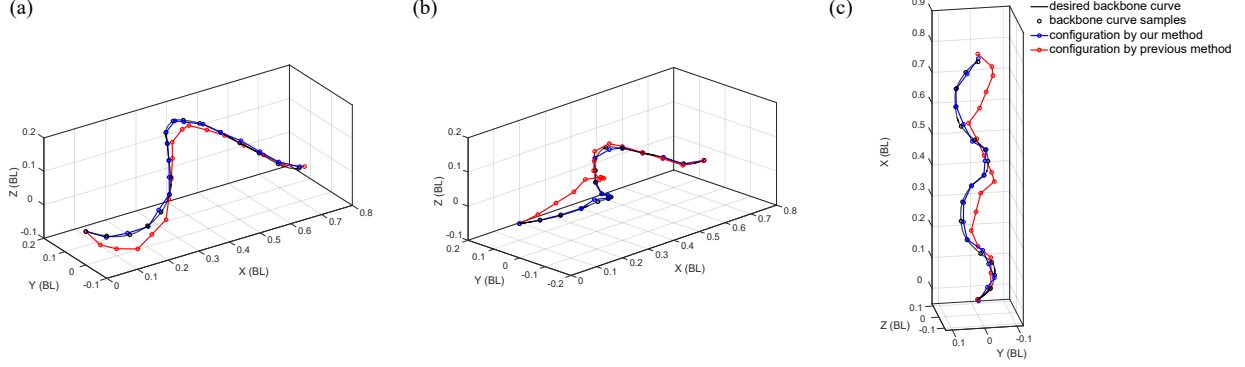


Fig. 2: Comparisons for the robot configurations by our method, the robot configurations by the previous method, and the desired backbone curves in (a) a sidewinding gait, (b) a sinus lifting gait, and (c) a helical rolling gait. Black curves are the desired backbone curves, blue and red piece-wise linear curves are robot configurations by our method and by the previous method, respectively. Black circles represent samples of the desired backbone curve, blue and red circles represent joints in corresponding robot configurations. All coordinates are normalized by the body length (BL) of the robot. Our reconstruction method allows more accurate curve-configuration conversions.

criterion $D = \sum_{i=0}^{n+1} \|C_i - C'_i\|^2$, where C_i are the positions for desired backbone curve samples and C'_i are the positions of the joints and two ends of the robot.

1) *Sidewinding*: The desired finite-length continuous backbone curves in 3-D Cartesian space for sidewinding were achieved with parametric equations.

$$\begin{aligned} y &= A_y \sin(\omega_y x + ft) \\ z &= A_z \sin(\omega_z x + ft + \phi), \end{aligned} \quad (2)$$

where we fixed $x \in [0, 1]$, $A_y = \pi/4$, $A_z = \pi/3$, $\omega_y = \omega_z = 2\pi$, $f = 1$, and $\phi = -\pi/2$. A sequence of 200 backbone curve examples in a gait cycle were then achieved by varying t . A comparison of the robot configuration by our method, the robot configuration by the previous method, and the desired backbone curve is shown in Fig. 2(a), the coordinates are normalized by the body length of the robot (BL). For the 200 backbone curve examples, the averaged sum of squares distances error for the robot configurations by our method is $0.0010 \pm 0.0003 \text{ BL}^2$, while the averaged sum of squares distances error for the robot configurations by the previous method is $0.0579 \pm 0.0378 \text{ BL}^2$, as illustrated in Fig. 3.

2) *Sinus lifting*: We achieved sinus lifting backbone curves by setting the parameters in (2) as $x \in [0, 1]$, $A_y = A_z = \pi/4$, $\omega_y = 2\pi$, $\omega_z = 3\pi$, $f = 1$, and $\phi = \pi/2$. Similar to the method described in the previous section, we performed comparisons over 200 backbone curve examples, one of which is as depicted in Fig. 2(b). The average of the sum of squares distances error for the robot configurations by our method is $0.0007 \pm 0.0002 \text{ BL}^2$, which is much smaller than the robot configurations by the previous method $0.0510 \pm 0.0297 \text{ BL}^2$, as shown in Fig. 3.

3) *Helical rolling*: Backbone curves for a helical rolling gait can also be achieved with parameters $x \in [0, 1]$, $A_x = A_y = \pi/3$, $\omega_x = \omega_y = 4\pi$, $\phi = \pi/2$, and $f = 1$ in (2). A sequence of 200 desired backbone curve examples covering a full gait cycle were collected by varying t in the same manner used in previous sections. The comparison between an example of the desired curve and the robot configurations is demonstrated in Fig. 2(c). The robot configurations by

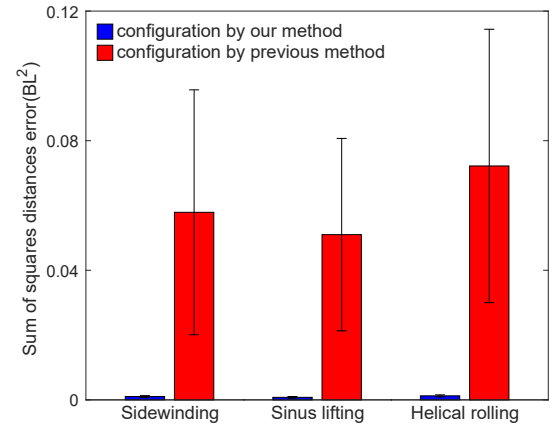


Fig. 3: A comparison of averaged discrepancies between the robot configurations and the desired backbone curves for selected sidewinding, sinus lifting and helical rolling gaits among 200 backbone curve examples on the virtual robot model. Discrepancies are evaluated by the sum of squares distances error between the positions of the robot's joints and the positions of corresponding samples on the desired backbone curve. Blue bars represent robot configurations by our method, and red bars represent robot configurations by the previous method. Error bars indicate the standard deviation. The configurations by our method have much smaller sum of squares distances error to the desired backbone curves than the configurations by the previous method.

our method achieve a $0.0012 \pm 0.0003 \text{ BL}^2$ averaged sum of squares distances error to the desired curves over 200 examples, while the number for the robot configurations by the previous method is $0.0747 \pm 0.0422 \text{ BL}^2$, as shown in Fig. 3.

Much smaller discrepancies between the configurations by our method and desired backbone curves shown in the three selected gait examples indicate that our reconstruction method improves the quality of curve-configuration conversions, i.e., the robot body can better approximate the desired backbone curves. We also found that the reconstruction process for each desired curve can be completed within 0.2s, which allows us

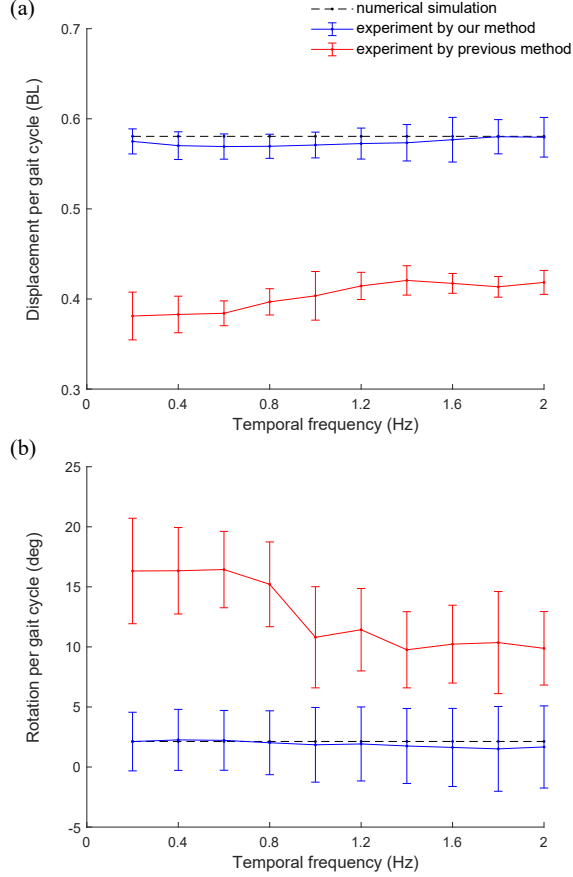


Fig. 4: The body displacement and body rotation of the robot over a gait cycle for the sidewinding gaits with different temporal frequencies. The dashed black lines are the numerical predictions. The blue lines are the mean values of five experiment trials for the gaits by our method, and the red lines are for the gaits by the previous method. The error bars are standard deviations. The robot can achieve larger body displacement and less body rotation with our method. The agreement between the locomotive performances of the gait by our method and the numerical predictions suggests that our method allows the discrete robot to realize the desired motion of the sequence of continuous backbone curves.

to implement this method in real-time robot locomotion.

B. Real-time implementation in physical robot locomotion

We performed the reconstruction method in real-time to create joint angle set-points for a snake robot. In the following robot experiments, a snake robot composed of sixteen identical actuated one DOF bending joints was used, as shown by Fig. 1. The joints are arranged such that the neighboring modules' axes of rotation are torsionally rotated ninety degrees relative to each other, yielding an alternative-pitch-and-yaw twist-free geometry. In each joint, a low-level PID controller is embedded, which controls the actuators to follow the joint angle set points. Experiments were conducted on flat, smooth, hard ground, where we assume the ground reaction forces are given by kinetic Coulomb friction. For each experiment, we conducted five trials for each gait tested, and we commanded the snake robot to execute two full gait cycles for each trial. We tracked the snake robot's trajectory via eight reflective

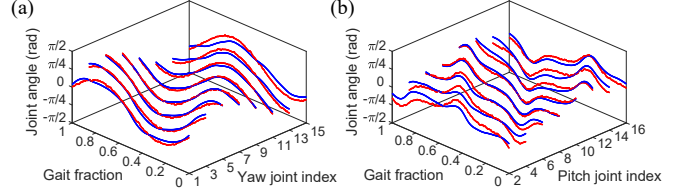


Fig. 5: A comparison of output joint angle trajectories for the same sequence of backbone curves by different optimization algorithms for the sidewinding gait with $f = 1\text{Hz}$. Blue trajectories are achieved by running the “annealed chain fitting” method of [8]. Red trajectories are achieved by running the proposed optimization algorithm in this work. The joint angle trajectories output by the method we proposed in this work are smooth, which are able to be used directly on the robot to produce a continuous locomotion, while the joint angle trajectories by the previous method are not smooth, which need a post-processing step of smoothing.

markers attached evenly along the backbone of the robot and an OptiTrack motion capture system.

To test the effectiveness of our reconstruction method in real-time, we conducted experiments of the robot executing a series of sidewinding gaits with varying temporal frequencies (gait speeds) with the our reconstruction method implemented, and with the previous method implemented, respectively. Following the gait design reported in [14], desired 3-D backbone curves were composed by sinusoidal waves in horizontal plane and sigmoid-filtered sinusoidal waves in vertical plane, prescribed by

$$\begin{aligned} y &= A_y \sin(\omega_y x + ft) \\ z &= A_z \sigma[\sin(\omega_z x + ft + \phi)], \end{aligned} \quad (3)$$

where $\sigma(t) = \frac{1}{1+e^{-\gamma t}}$. We fixed $\gamma = 4$, $A_y = \pi/4$, $A_z = \pi/3$, $\omega_y = \omega_z = 2\pi$, and $\phi = -\pi/2$. We varied the temporal frequency $f \in (0, 2]$ Hz to achieve a family of sidewinding gaits with different gait speeds to test the real-time performance of our method.

To make sure that the joint angle sequence output by our optimization algorithm can produce a continuous locomotion of the robot, we first examined the smoothness of joint angle trajectories and compared them with the joint angle trajectories output by an optimization method called *annealed chain fitting* introduced in [8] given the same sequence of backbone curves. Fig. 5 visualized the joint angle trajectories by two methods. We calculated the averaged difference between neighbouring joint angles over the chronological sequence of 200 robot configurations in a full gait cycle. We found that the previous method resulted in an average joint angle change between time steps of 10.42 degrees, whereas our method resulted in only 1.64 degrees change between time steps. This comparison demonstrated the joint angle trajectories output by the previous method are not smooth, so that they require a post-processing smoothing step. The trajectories output by our method do not need a smoothing step and can be used directly on the robot to produce a continuous motion.

We then studied the robot's locomotion by measuring the robot's body displacement and body rotation. We compared the motion of the gaits by our method and the gaits by the

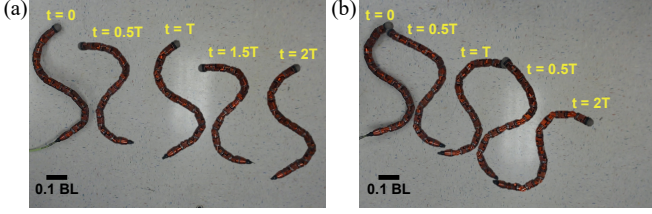


Fig. 6: Video frame sequences of the robot experiments of the sidewinding gait at $f = 1\text{Hz}$ (a) with our reconstruction method, and (b) with the previous method. The desired motion for the robot is to translate from left to right without body rotating. Here time t is measured in terms of complete gait cycle period T .

previous method with the desired motion from a numerical prediction. In the numerical prediction, the contact state pattern is prescribed with the assumption that the robots' configuration is a 3-D continuous curve [24]. The displacement is calculated by numerically integrating the equations of motion for the continuous curve throughout one period based on the resistive force theory [25], [26], which has been demonstrated as a reliable method to provide predictions for snake robot locomotion [13], [27], [28]. Fig. 4 shows the quantitative results of the robot's body displacement and body rotation over a gait cycle versus temporal frequency f . We found that the robot's body displacement and body rotation with our method agree with the numerical predictions, which indicates our method allows the discrete robot to approach the performance of a desired motion of a sequence of desired continuous backbone curves. In contrast, the robot's body displacement of gaits by the previous method cannot reach the predictions, and large unexpected body rotation emerges during the gait cycle. The results also demonstrated that the reconstruction method enables the robot to perform robustly over different temporal frequencies (gait speeds) as predicted, while the robot's locomotion with the previous method vary as temporal frequency changes. Video frame sequences of the robot experiments of executing the gaits by our method and by the previous method with $f = 1\text{Hz}$ is shown in Fig. 6, which illustrate that the gait by our method generates larger body displacement and less body rotation.

To further investigate how our reconstruction method impacts the robot's locomotion, we compared the robot's contact state patterns during a gait cycle with the desired contact state pattern that generated by the numerical prediction of the desired gait. We obtained the contact state patterns for the gaits with our method and the gaits with the previous method from the tracked motion data. At each time step, if a marker's height lied below the average of height of the tracking markers, we considered its corresponding body section to be in contact with the ground; otherwise, we considered the body section of the robot to be not in contact. We found that the contact state patterns for the gaits by our method share a high similarity with the desired contact state patterns with an averaged 89.4% percentage overlap, while the number for the gaits by the previous method is 57.2%, examples of contact state patterns can be found in Fig. 7. This comparison indicates that the reconstruction method allows more accurate conversions from

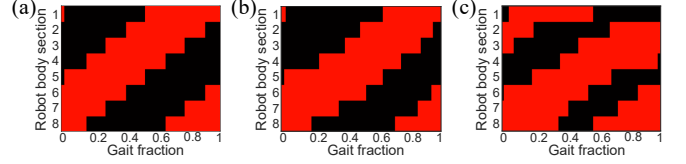


Fig. 7: (a) The desired contact state pattern of the robot determined by the desired sidewinding gait at $f = 1\text{Hz}$, (b) the contact state pattern of the robot executing the gait by our method, and (c) the contact state pattern of the robot executing the gait by the previous method. The contact state pattern of the gait by our method shares a higher similarity (89.4%) with the desired contact state pattern than the gait by the previous method (57.2%).

the desired backbone curves to robot configurations, so that the robot can achieve a contact state pattern shares higher similarity with the desired pattern, which in turn enables the robot to achieve the desired locomotion of a sequence of desired continuous backbone curves.

V. CONCLUSION

In this paper, we presented a reconstruction method that can realize 3-D continuous backbone curve on discrete snake robots with a twist-free alternating pitch and yaw joints design. Our analysis showed that our method allows more accurate curve-configuration conversions than the previous method by applying them to the backbone curve examples for three types of widely used gaits in snake robot locomotion. We also conducted physical robot experiments to compare the reconstruction method and the previous method, in which the robot was commanded to execute a family of sidewinding gaits with different temporal frequencies. We experimentally validated our optimization algorithm enables that small changes in the desired backbone curves only result in small changes in the robot configuration, which lead to continuous robot locomotion. By comparing the body displacement and rotation, we found that the gaits by our method outperform the gait by the previous method, generating larger body displacement and less body rotation. Furthermore, we verified the robot's locomotive performances and contact state patterns of executing the gaits by our method match with the numerical prediction of the desired motion generated by a sequence of desired continuous backbone curves, while the gaits by the previous method do not. Therefore, our reconstruction method offers promise in producing accurate conversions from the desired continuous backbone curves to discrete robot configurations and allowing the twist-free robot with robust, simple, single-axis rotary joints to achieve the desired agile locomotion of a sequence of continuous backbone curves.

The proposed reconstruction method focuses on the specific snake robot design of alternating pitch and yaw joints. Future work will investigate the extension of this idea to the applications on other twist-free mobile limbless robots and continuum manipulators. Further, we hope to integrate the reconstruction method into the shape-based compliant control framework for snake robot locomotion [29], [30], where it can help the robot comply to challenging 3-D terrains and irregular 3-D obstacles.

REFERENCES

- [1] C. Wright, A. Johnson, A. Peck, Z. McCord, A. Naaktgeboren, P. Gianfortoni, M. Gonzalez-Rivero, R. Hatton, and H. Choset, "Design of a modular snake robot," in *2007 IEEE/RSJ International Conference on Intelligent Robots and Systems*. IEEE, 2007, pp. 2609–2614.
- [2] S. Takaoka, H. Yamada, and S. Hirose, "Snake-like active wheel robot acm-r4. 1 with joint torque sensor and limiter," in *2011 IEEE/RSJ International Conference on Intelligent Robots and Systems*. IEEE, 2011, pp. 1081–1086.
- [3] A. A. Transeth, R. I. Leine, C. Glocker, K. Y. Pettersen, and P. Liljebäck, "Snake robot obstacle-aided locomotion: Modeling, simulations, and experiments," *IEEE Transactions on Robotics*, vol. 24, no. 1, pp. 88–104, 2008.
- [4] Q. Fu, S. W. Gatt, T. W. Mitchel, J. S. Kim, G. S. Chirikjian, and C. Li, "Lateral oscillation and body compliance help snakes and snake robots stably traverse large, smooth obstacles," *Integrative and Comparative Biology*, 2020.
- [5] M. Nilsson, "Why snake robots need torsion-free joints and how to design them," in *Proceedings. 1998 IEEE International Conference on Robotics and Automation (Cat. No. 98CH36146)*, vol. 1. IEEE, 1998, pp. 412–417.
- [6] S. Hirose, "Biologically inspired robots," *Snake-Like Locomotors and Manipulators*, 1993.
- [7] G. S. Chirikjian and J. W. Burdick, "A modal approach to hyper-redundant manipulator kinematics," *IEEE Transactions on Robotics and Automation*, vol. 10, no. 3, pp. 343–354, 1994.
- [8] R. L. Hatton and H. Choset, "Generating gaits for snake robots: annealed chain fitting and keyframe wave extraction," *Autonomous Robots*, vol. 28, no. 3, pp. 271–281, 2010.
- [9] T. Takemori, M. Tanaka, and F. Matsuno, "Gait design for a snake robot by connecting curve segments and experimental demonstration," *IEEE Transactions on Robotics*, vol. 34, no. 5, pp. 1384–1391, 2018.
- [10] J. W. Burdick, J. Radford, and G. S. Chirikjian, "A'sidewinding'locomotion gait for hyper-redundant robots," in *[1993] Proceedings IEEE International Conference on Robotics and Automation*. IEEE, 1993, pp. 101–106.
- [11] S. Ma, Y. Ohmameuda, and K. Inoue, "Dynamic analysis of 3-dimensional snake robots," in *2004 IEEE/RSJ International Conference on Intelligent Robots and Systems (IROS)(IEEE Cat. No. 04CH37566)*, vol. 1. IEEE, 2004, pp. 767–772.
- [12] M. Tesch, K. Lipkin, I. Brown, R. Hatton, A. Peck, J. Rembisz, and H. Choset, "Parameterized and scripted gaits for modular snake robots," *Advanced Robotics*, vol. 23, no. 9, pp. 1131–1158, 2009.
- [13] H. C. Astley, C. Gong, J. Dai, M. Travers, M. M. Serrano, P. A. Vela, H. Choset, J. R. Mendelson, D. L. Hu, and D. I. Goldman, "Modulation of orthogonal body waves enables high maneuverability in sidewinding locomotion," *Proceedings of the National Academy of Sciences*, vol. 112, no. 19, pp. 6200–6205, 2015.
- [14] B. Zhong, T. Wang, J. Rieser, A. Kaba, H. Choset, and D. Goldman, "Frequency modulation of body waves to improve performance of limbless robots," in *Robotics: Science and Systems*, 2020.
- [15] B. O'Neill, *Elementary differential geometry*. Academic press, 2014.
- [16] G. S. Chirikjian and J. W. Burdick, "The kinematics of hyper-redundant robot locomotion," *IEEE transactions on robotics and automation*, vol. 11, no. 6, pp. 781–793, 1995.
- [17] H. Mochiyama, E. Shimemura, and H. Kobayashi, "Shape control of manipulators with hyper degrees of freedom," *The International Journal of Robotics Research*, vol. 18, no. 6, pp. 584–600, 1999.
- [18] S. B. Andersson, "Discretization of a continuous curve," *IEEE Transactions on Robotics*, vol. 24, no. 2, pp. 456–461, 2008.
- [19] M. Tanaka and F. Matsuno, "A study on sinus-lifting motion of a snake robot with switching constraints," in *2009 IEEE International Conference on Robotics and Automation*. IEEE, 2009, pp. 2270–2275.
- [20] W. Zhen, C. Gong, and H. Choset, "Modeling rolling gaits of a snake robot," in *2015 IEEE International Conference on Robotics and Automation (ICRA)*. IEEE, 2015, pp. 3741–3746.
- [21] MATLAB, *version 9.8.0 (R2020a)*. Natick, Massachusetts: The MathWorks Inc., 2020.
- [22] J.-B. Lasserre, *Moments, positive polynomials and their applications*. World Scientific, 2010, vol. 1.
- [23] D. Rollinson and H. Choset, "Gait-based compliant control for snake robots," in *2013 IEEE International Conference on Robotics and Automation*. IEEE, 2013, pp. 5138–5143.
- [24] H. C. Astley, J. R. Mendelson, J. Dai, C. Gong, B. Chong, J. M. Rieser, P. E. Schiebel, S. S. Sharpe, R. L. Hatton, H. Choset, *et al.*, "Surprising simplicities and syntheses in limbless self-propulsion in sand," *Journal of Experimental Biology*, vol. 223, no. 5, 2020.
- [25] R. L. Hatton and H. Choset, "Nonconservativity and noncommutativity in locomotion," *The European Physical Journal Special Topics*, vol. 224, no. 17, pp. 3141–3174, 2015.
- [26] C. Li, T. Zhang, and D. I. Goldman, "A terradynamics of legged locomotion on granular media," *science*, vol. 339, no. 6126, pp. 1408–1412, 2013.
- [27] T. Wang, B. Chong, K. Diaz, J. Whitman, H. Lu, M. Travers, D. I. Goldman, and H. Choset, "The omega turn: a biologically-inspired turning strategy for elongated limbless robots," in *2020 IEEE/RSJ International Conference on Intelligent Robots and Systems (IROS)*. IEEE, 2020, pp. 000–000.
- [28] B. Chong, Y. O. Aydin, C. Gong, G. Sartoretti, Y. Wu, J. M. Rieser, H. Xing, J. W. Rankin, K. Michel, A. G. Nicieza, *et al.*, "Coordination of back bending and leg movements for quadrupedal locomotion," in *Robotics: Science and Systems*, 2018.
- [29] M. J. Travers, J. Whitman, P. E. Schiebel, D. I. Goldman, and H. Choset, "Shape-based compliance in locomotion," in *Robotics: Science and Systems*, 2016.
- [30] T. Wang, J. Whitman, M. Travers, and H. Choset, "Directional compliance in obstacle-aided navigation for snake robots," in *2020 American Control Conference (ACC)*, 2020, pp. 2458–2463.